MICROSTRUCTURAL DEVELOPMENT DURING SINTERING OF PM STEELS WITH ADMIXED NICKEL

S. Sainz, W. García, A. Karuppannagounder, F. Castro

ABSTRACT
Sintering diffusion bonded powder mixtures generally leads to high strength steels with heterogeneous microstructures. In particular, the presence of nickel-rich regions is widely reported, although a detailed description of the mechanisms leading to their formation is scarcely documented. This work reports on the microstructural development during sintering of a Fe-0.8 wt.% Mo prealloyed powder containing admixed nickel. Changes induced by using ultra-fine nickel instead of a coarser grade have also been studied. It is demonstrated that the formation of nickel rich-regions is the result of limited nickel redistribution by diffusion. Against conventional thinking it is demonstrated that the formation of nickel rich-regions is based on Ni diffusion through the (Fe-Mo-C) austenite grain boundaries followed by the interdiffusion between the iron-based and Ni particles with preferential diffusion of Fe into nickel.
Keywords: nickel-rich regions, heterogeneous microstructures

INTRODUCTION

Over the years, and amongst other factors associated to new equipments and processes, the growth of ferrous PM has been particularly linked to the development of new powders and powder blends [1,2]. One of the most favoured alloy systems for high load applications is based on blends prepared by diffusion bonding Ni and Cu particles onto Fe-Mo prealloyed powders [2,3]. The steels are classed as sinter-hardening grades and exhibit heterogeneous microstructures after sintering. In particular, the presence of nickel-rich regions is widely reported [4-12] although a detailed description of the mechanisms for their formation is scarcely documented. These “Ni-rich regions” have a marked influence on mechanical properties [6-14] and dimensional tolerances [15]. Typical diffusion bonded powder blends contain up to 4 wt.% Ni additions to prealloyed Fe-1.5 wt.% Mo [16,17]. However, leaner alternative powder mixtures containing 0.8 wt.% Ni [18] or even 0.5% Ni [19] have been recently proposed.

Recent studies [20-22] illustrate the advantages of using extra-fine Ni particles instead of the typically coarser grades. Upon cooling from the sintering temperature a larger amount of martensite was observed. An increased diffusion rate of nickel was suggested as an explanation [20,21]. The present work includes a detailed description of the diffusion events leading to the formation of nickel-rich areas. Evidence is provided, against conventional thinking, which indicates that heterogeneous microstructures are not only the result of a slow volume diffusion of nickel into iron but that the preferential atom flow is from iron into nickel.

Shandra Sainz, Wilfredo García, Arulkumar Karuppannagounder, Francisco Castro, CEIT, San Sebastián, Spain

EXPERIMENTAL PROCEDURE

The experimental powder compacts were prepared using Ancorsteel 85HP as the Fe-base powder to which 0.5-0.6 wt.% graphite and, 0.8 or 10 wt.% Ni were added. The nickel grades used were INCO 123 with a mean particle size < 7 μm and ultra-fine nickel, prepared by Eurotungstène with a mean particle size < 0.5 μm. Specimens containing 0.8 wt.% nickel were sintered at 1120ºC for 1 h, cooled at 3.75ºC/s under high pressure inert gas and tempered during 30 min at 300ºC. Specimens containing 10% nickel (INCO 123) additions were specially prepared to study the microstructural evolution and alloy development. Interrupted sintering experiments followed by immediate water quenching were performed. The heating rate in all cases was 20ºC/min. The microstructures were observed under the optical and scanning electron microscope fitted with energy dispersive spectroscopy (EDS) facilities. The SEM micrographs were taken using the backscattered electron detector.

RESULTS AND DISCUSSION

Figures 1a and b show the microstructures of two sintered specimens containing 0.8% Ni from typical and ultra-fine grades, respectively. Complementarily, as illustrated by the SEM micrographs and the EDS line scan in Fig.2, the concentration of nickel, along the horizontal test line arrowed in the micrographs, clearly fluctuates while Mo remains fairly constant. As observed from Fig.2a, the specimen with the coarser nickel grade shows that the featureless areas in light contrast correspond to the highest concentration of nickel. According to the quantitative EDS analyses carried out the maximum nickel concentration found in those areas was between 30 and 40 wt.%, the rest, apart from carbon, being Mo (~ 0.8 wt.%) and iron. Inspection of Fig.2b, allows realising that the fluctuation in the concentration of nickel is still observed although the variations are more attenuated than in the previous case.

From these micrographs it is observed that after accelerated cooling and tempering the microstructure of these sintered steels are heterogeneous. The microstructure in Fig.1a consists of a combination of bainitic grains, another constituent in dark contrast corresponding to tempered martensite and some featureless areas in light contrast corresponding to austenite. Figure 1b shows a more uniform microstructure containing bainitic and tempered martensite areas without clearly noticeable light contrast areas. It is consequently seen that using ultra-fine nickel additions clearly leads to a more uniform distribution of this alloying element thus promoting grain refinement and a dispersion of martensite areas throughout the microstructure.

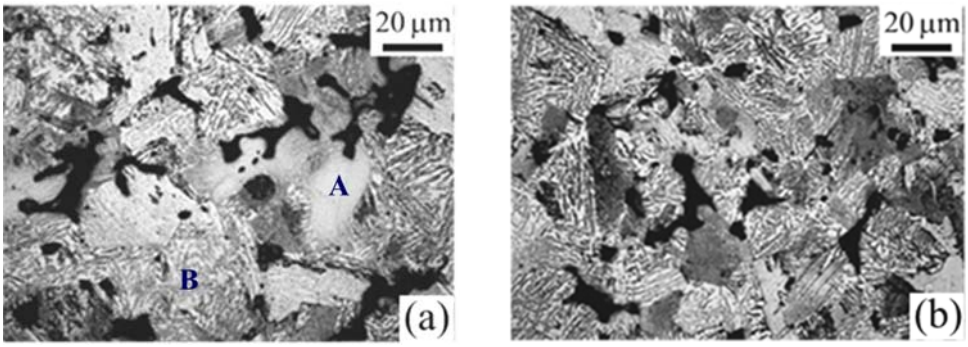

Fig.1. Optical micrographs from tempered specimens containing 0.8 wt.% Ni+0.5% graphite. The powder mixtures contain admixed (a) fine Ni and (b) ultra-fine Ni. A and B mean austenite and bainite respectively.

However, the line scan traces in Fig.2 show that the microstructure is still chemically heterogeneous exhibiting fluctuating nickel concentrations that maintain the Ni-rich regions although at a much shorter range, and more diluted, than those observed after using coarser Ni particles. Also, the mere fact that the samples exhibit a variety of phases after accelerated cooling intrinsically indicates local variations in chemical composition thus leading to areas of different local hardenability.

Hence, although the more evident nickel concentration is associated to the light contrast areas, it must be understood that nickel, being unevenly distributed, exerts an important influence on the overall microstructural development. The bainitic areas are clearly associated with nickel minima. In this sense these areas correspond to the unalloyed (except for carbon) remnants of the original iron-base particles. On the other hand, in areas where nickel rises in concentration it can certainly lead to the formation of martensite or even austenite as is well known from the constitutional diagrams for Ni steels [23].

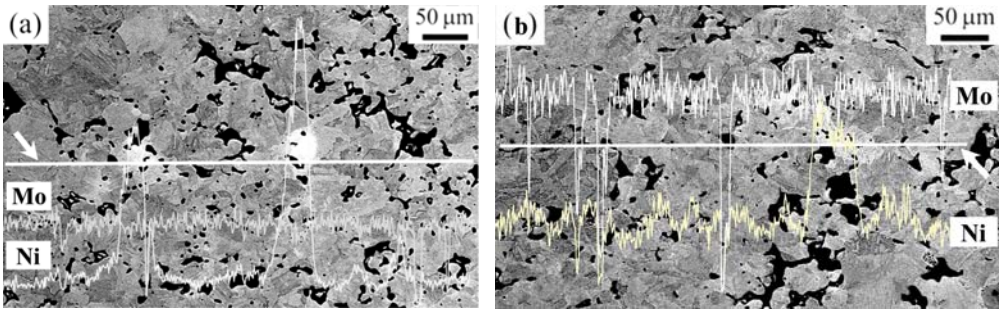

Fig.2. SEM micrographs and line scan traces, for Mo and Ni, from tempered specimens containing 0.8 wt.% Ni+0.5% graphite; using (a) fine Ni and (b) ultra-fine Ni.

To acquire a detailed appreciation of the mechanisms involved in the redistribution of nickel and the formation of nickel-rich areas, a special set of specimens containing 10 wt.% nickel were studied after interrupted sintering experiments. Figure 3a shows the appearance of the microstructure after heating to 900ºC. Apart from the porosity, the microstructure is constituted by nickel located around the Fe-base particles which exhibit a martensitic structure due to the presence of carbon in solution. Although the nickel particles are still clearly recognisable an advanced sintering state is observed with extensive neck formation between them. This high sinter-activity may be expected from the large surface area associated to their morphology and small particle size. But, up to this temperature the interaction between the nickel and Fe particles is still very limited.

In contrast, after quenching from 1120ºC, Figs.3b and c show the formation of a continuous nickel network surrounding the iron-base particles and nickel diffusion through the prior austenite grain boundaries (as arrowed on the micrographs) with the consequent fragmentation of the Fe-particles. This result is in excellent agreement with the observations by Puckert et al. [24] in their work with nickel coated Fe particles. Finally, Fig.3d shows the microstructure of a specimen sintered for 15 min at 1120ºC followed by furnace cooling. It is constituted by pearlitic areas, corresponding to the remnants of the Fe-Mo-C particles, exhibiting rims around them of the same microstructure as the extended areas showing a bainite-like structure consisting of a ferrite matrix and a dispersion of cementite. A third continuous and structureless constituent exhibiting light contrast is also clearly observed.

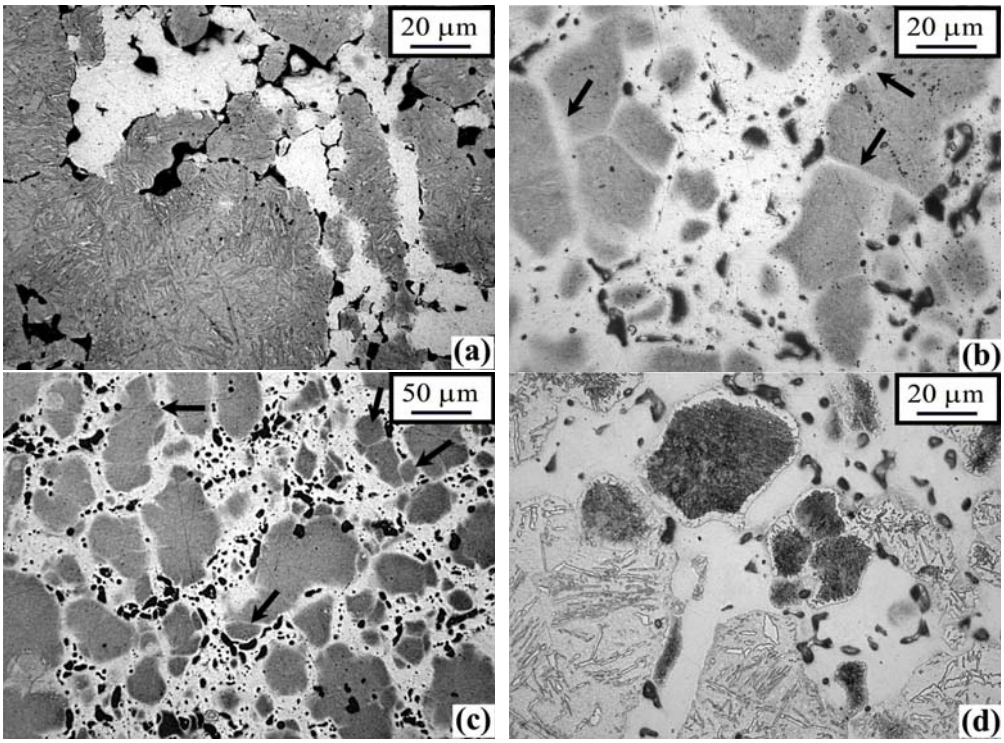

Fig.3. Optical micrographs of 85HP+0.6% graphite+10% Ni quenched from (a) 900ºC, (b,c) 1120ºC, and (d) sintered at 1120ºC for 15 min and furnace cooling.

The reason for the uneven distribution of nickel and the formation of the nickel-rich areas can thus be understood from the sequence of events illustrated by Fig.3. As noticed, after the limited interaction between the nickel and Fe-base particles at 900ºC (Fig.3a) important changes start taking place during heating at a temperature between 900º and 1120ºC (Fig.3b and c). Figures 3b and c exhibit several aspects worth mentioning. Firstly, after extensive neck development between the nickel particles, nickel forms a continuous phase as a result of spreading around the Fe particles by rapid surface diffusion at these intermediate temperatures. This has also been suggested before by Hwang et al. [12]. Secondly, the great majority of the porosity is found within these nickel regions as a result of constrained shrinkage due to sintering of a dual particle size distribution system, since the mean particle size of the prealloyed Fe-Mo powder is around ten times larger than that of nickel. As a result a change in the morphology, size and amount of porosity can be clearly appreciated. Thirdly, the interaction between the nickel and Fe-base particles is clearly taking place as nickel forms a continuous network around them. Intensive nickel diffusion along the prior austenite grain boundaries is evidenced as indicated by the arrows in Fig.3b. Taking place at the contact points this leads to the fragmentation of the iron particles so that small Fe-base fragments are embedded in the continuous nickel network. Also, as observed from the low magnification view in Fig.3c, the microstructure is characterised by the presence of larger iron-base areas. These correspond to the remnants of the initially larger particles, since it must be realised that the high concentration of nickel at the surface falls to negligible levels inside them. This may also be expected since the austenite grains located at their interiors are subjected to fast growth [25] while nickel grain

boundary diffusion simultaneously takes place at the periphery. In this sense it may be deduced that penetration of nickel through the grain boundaries only affects a few micrometers from their surface since austenite grain growth limits grain boundary diffusion, hence counteracting fragmentation, by decreasing the number of grain boundaries available.

Additionally, as noticed in Fig.3b, the large D_b/D_v ratio [26] results in rapid nickel transport through the grain boundaries and slow diffusion into the adjacent volume. As a consequence after nickel grain boundary diffusion, the surrounded Fe-base grains pass to be embedded in the continuous nickel phase. Further progress of the microstructure tending to smooth out chemical gradients thus requires volume diffusion.

Before analysing this effect it is convenient to recall that in the Fe-Ni alloy system the binary phase diagram shows a continuous solid solution for Fe-Ni at all Ni concentrations in a wide range of temperatures. Additionally, their atomic radii and lattice parameter in the FCC form are very similar. Hence, it may be reasonably expected that alloying in this system will take place by the interdiffusion of both substitutional elements. But, against current believe [8,10,11,20-22], this takes place with preferential diffusion of Fe into nickel. This statement is also supported by the values of the intrinsic diffusion coefficients of iron into nickel (D_{Fe}) and vice versa (D_{Ni}) reported in the Landolt-Börnstein tables [26]. It must be emphasised that $D_{Fe} > D_{Ni}$ in about one order of magnitude at all temperatures and compositions in the Fe-Ni alloy system. As an example $D_{Fe} \sim 1.6.10^{-14}$ m^2/s at 1409 K in pure nickel. This sense of diffusion has also been recently confirmed by noticing that the Matano interface, after heating of Fe-Ni diffusion pairs, was always located at an iron concentration of 40±2 at % [27]. The same workers demonstrated that regardless of pressure and temperature the obtained diffusion profiles were always asymmetric, indicating larger penetration distances of Fe into Ni in more than 60% as compared to those of nickel into iron.

It may therefore be understood that the formation of nickel-rich regions frequently observed in powder metallurgy is a consequence of the relatively slow volume diffusion of iron into nickel, which is in fact the rate controlling step for chemical homogenisation. As iron is incorporated in nickel from the surface of the Fe-base particles, and particularly from the small isolated grains after fragmentation, very pronounced compositional gradients are formed. This situation is well illustrated by Fig.3d which shows the microstructure of the same material but sintered at 1120ºC for 15 min followed by furnace cooling. The slow cooling tends to produce the equilibrium structure which, as observed, is still clearly heterogeneous even after a longer period at high temperature. The microstructure is characterised by the formation of several transformation products which evidence the existence of chemical gradients that influence local hardenability. A continuous “ligther contrast” structureless area corresponding to nickel-rich austenite (containing around 30-40 wt.%) is clearly recognisable surrounding areas with the appearance of pearlite which do not contain Ni, and larger blocks where coarse bainite or Widmanstätten ferrite growth is observed in a martensite matrix. This latter bainitic structure, which may also be identified forming rims around the areas with pearlitic aspect, is now occupying the largest volume fraction in the microstructure and may be formed as a result of carbon and nickel partitioning during slow cooling as described by Bhadeshia [28] and Reynolds et al. [29].

Finally, it is important to consider that using large nickel particles and/or large amounts of admixed nickel will favour the formation of a rising nickel concentration profile from the periphery of the Fe-based particles to the centre of the nickel areas. In contrast, using small nickel particles and small nickel amounts will tend to give smoother nickel

profiles. But due to the slow alloying process complete homogenisation of the alloy may require high temperature sintering or very long sintering times. As evidenced by Fig.1b, the use of ultra-fine nickel additions leads to obtaining higher amounts of martensite since, as described above, the resulting nickel rich areas will be smaller and more diluted in Ni. However, it must be emphasized that the value of the diffusion coefficients are not altered by using different particle sizes.

CONCLUSIONS

Summarising it may be concluded that PM steels containing admixed nickel exhibit heterogeneous microstructures after sintering at 1120ºC because of the formation of nickel-rich regions as a result of the slow volume diffusion of iron into nickel. Their formation is based on: surface diffusion of nickel around the Fe-base particles, fast but limited nickel grain boundary diffusion through the austenite grain boundaries and slow volume interdiffusion of Fe and Ni with preferential flow from iron into nickel. The Ni gradient thus generated favours the formation of “unalloyed” regions at the centre of the prior Fe-based particles as well as regions with medium and high nickel contents. The final microstructure may consist of particular combinations of phases with pearlite appearance, bainite, martensite and austenite. The use of ultra-fine nickel particles leads to a more uniform distribution of nickel but does not remove completely the compositional and microstructural heterogeneity.

Acknowledgements

The authors acknowledge Eurotungstène for providing the ultra-fine nickel powder.

REFERENCES

[1] Pickering, S.: Metal Powder Report, 1998, no. 1, p. 16
[2] James, WB.: The Int. J. of Powder Metallurgy, vol. 30, 1994, no. 2, p. 157
[3] Capus, JM.: Metal Powder Report, 1997, September, p. 17
[4] Lindskog, P.: Powder Metallurgy, vol. 13, 1970, no. 26, p. 280
[5] Terchek, RL., Hirschhorn, JS. In: Proc. of Third European PM Symposium. Brighton, England, 1971, p. 9
[6] Svensson, LE.: Powder Metallurgy, vol. 17, 1974, no. 34, p. 271
[7] Fulkner, RG., Burr, DJ.: Powder Metallurgy International, vol. 10, 1978, no. 1, p. 24
[8] Khaleghi, M., Haynes, R.: Powder Metallurgy, vol. 28, 1985, no. 4, p. 217
[9] Douib, N., Mellanby, IJ., Moon, JR.: Powder Metallurgy, vol. 32, 1989, no. 3, p. 209
[10] Zhang, H., German, R.: The Int. J. of Powder Metallurgy, vol. 27, 1991, no. 3, p. 249
[11] Degoix, CN., Griffo, A., German, RM.: The Int. J. of Powder Metallurgy, vol. 34, 1998, no. 6, p. 57
[12] Hwang, KS., Hsieh, CH., Shu, GJ.: Powder Metallurgy, vol. 45, 2002, no. 2, p. 160
[13] Tunstall, J., Haynes, R.: The Int. J. of Powder Metallurgy, vol. 16, 1980, no. 1, p. 69
[14] Hwang, KS., Wu, MW., Yen, FC., Sun, CC.: Materials Science Forum, vol. 534-536, 2007, p. 537
[15] Lindsley, B., Murphy, T. In: Proc. of Powder Met 2006. San Diego, USA, 2006, p. 140
[16] MPIF Standard 35. Materials Standards for PM Structural Parts. Princeton, NY, 2007, p. 40
[17] Höganäs iron and steel powders for sintered components. Höganäs, 1998, p. 151
[18] Sainz, S., García, W., Sarasola, M., Bonneau, M., Castro, F. In: Proc. of EuroPM 2007. Toulouse, France, 2007, p. 9
[19] Lindsley, B. In: Proc. of EuroPM 2007. Toulouse, France 2007, p. 107

[20] Stephenson, TF., Campbell, ST., Singh, T. In: Proc. of EuroPM 2003. Valencia, Spain, 2003, p. 269
[21] Campbell, ST., Singh, T., Stephenson, TF.: Advances in Powder Metallurgy & Particulate Materials, vol. 2, 2004, no. 7, p. 121
[22] Stephenson, TF., Singh, T., Sun, S., Wang, Z.: Advances in Powder Metallurgy & Particulate Materials, vol. 5, 2002, p. 153
[23] Hardbord, FW.: The metallurgy of steel. 7th ed. London : Griffin´s Metallurgical Series, 1923
[24] Puckert, J., Kaysser, WA., Petzow, G.: The Int. J. of Powder Metallurgy, vol. 20, 1984, no. 4, p. 301
[25] Sellars, CM., Whiteman, J.: Met. Sci., vol. 13, 1979, p. 187
[26] Landolt-Börnstein: Numerical data and functional relationships in science and technology. Ed. H. Mehrer. Vol. 26: Diffusion in solid metals and alloys. Berlin : Springer-Verlag, 1990
[27] Yunker, ML., Van Orman, JA.: Earth and Planetary Science Letters, vol. 254, 2007, p. 203
[28] Bhadeshia, HKDK.: Bainite in steels. 2nd ed. The Institute of Materials, 2000
[29] Reynolds, WT. Jr., Li, FZ., Shui, CK., Aaronson, HI.: Met. Trans. A, vol. 21A, 1990, p. 1443